Unsteady Flow and Heat Transfer in a Composite Porous Annulus with Time-Dependent Injection

Muhammad Nasir[a], Sufian Munawar[a,b], Ahmer Mehmood[c], and Asif Ali[a]

[a] Department of Mathematics, Quaid-i-Azam University, Islamabad, Pakistan
[b] Department of Mathematics, School of Science & Technology, University of Management & Technology, Lahore, Pakistan
[c] Department of Mathematics (FBAS), International Islamic University, Islamabad, Pakistan

Reprint requests to M. N.; Tel.: +92 313 5577676, E-mail: nasirmaths1@yahoo.com

Z. Naturforsch. **67a,** 657 – 664 (2012) / DOI: 10.5560/ZNA.2012-0068
Received February 6, 2012 / revised June 4, 2012 / published online October 17, 2012

In the present study, we deal with the momentum and heat transfer analysis in a horizontal annulus of a composite porous medium. The Darcy–Brinkman model is used to develop the governing equations for the flow and heat transfer phenomenon. The annulus injects the time dependent oscillatory velocity normal to its surface. Both the regions of the flow have their own viscosities, and the heat transfer analysis is carried out by retaining viscous dissipation. The governing equations for flow and heat transfer are solved analytically using a perturbation series for solutions in both regions of the annulus. A brief parametric analysis is performed for the velocity and the temperature profiles through graphs.

Key words: Unsteady Flow; Heat Transfer; Porous Medium; Suction/Injection.

1. Introduction

The study of porous channel flows and heat transfer has received tremendous attention during the past half century. This is because of the significance and diversity of this research area in various engineering and geophysical applications. One of such applications is in nuclear engineering in designing the pebble bed reactor. Also research on thermal reaction between heat generating porous bed and overlying fluid layer has largely been motivated by the nuclear reverse accident problem. Other applications also include filtration of water, porous bearings, bio convection in porous media, sewage, petroleum engineering, fault zone in geothermal systems, solid matrix heat exchangers, underground waste disposal in geotechnical engineering, and filter problems in chemical engineering. Unsteady oscillatory flows arise due to either unsteady motion of a boundary or boundary temperature. Such type of flow plays an important role in chemical engineering, turbo machinery, and aerospace technology.

The study of channel flow was initiated by Berman [1] who discussed steady two-dimensional laminar flow of a viscous fluid in a channel consisting of two porous walls. The Berman problem is further extended by various authors. Terrill [2] obtained the numerical solution of the Berman problem. Skalak and Wang [3] described multiple analytic solutions of the Berman problem. Terrill and Thomas [4] discussed fully-developed unidirectional laminar flow through a porous pipe. Rotating flow in a porous pipe was studied by Terrill and Thomas [5]. Marques et al. [6] extended the work of Terrill and Thomas [5] for Couette–Poiseuille flow in an annulus of infinite extent using similarity transformation. Taylor et al. [7] obtained the solution for three-dimensional flow in a porous channel. An analytic study was performed by Neale and Nader [8] to analyze the porous channel flow with slip condition. Moreover, the work was extended to various geometries and under different physical assumptions by authors of [9 – 13].

The study of flow through channels and ducts partially filled with a porous medium has profound implications in engineering and industrial processes. The theoretical learning on such kind of flows was done by authors of [8]. The analytical solutions for the study of fluid flow in the interfacial region between a porous medium and a clear fluid in channels partially filled with

a porous medium was discussed by Kuznetsov [14]. Kuznetsov [15] represents an analytical solution for the steady fully developed fluid flow in a composite region, which is partly filled with a porous medium and partly with a clear fluid and used stress jump boundary condition at the interface. Kuznetsov [16] discussed analytical solutions of Couette flow in a composite channel. Furthermore, Kuznetsov [17] investigated the fluid flow and heat transfer analysis of Couette flow in a composite duct. The problem of transient free convection in domains partially filled with porous substrates was investigated analytically by Al-Nimr and Khadrawi [18]. Chauhan and Kumar [19] discussed the effects of slip condition on forced convection and entropy generation in a circular channel by using the Darcy extended Brinkman–Forchheimer model. The effects of slip and other parameters were examined on the Nusselt number and entropy generation rate. Chauhan and Agrawal [20] studied the effects of Hall current on magnetohydrodynamic (MHD) fluid flow in a channel which was partially filled with a porous medium. The analytical solution for the study of unsteady radiation effects on natural convection MHD flow in a rotating vertical channel is examined by Chauhan and Rastogi [21]. Also Chauhan and Kumar [22] analyzed three dimensional Couette flows in a composite channel which is partially filled with a porous medium. Kuznetsov [23] considered fully developed forced convection in a parallel-plate channel partly filled with a homogenous porous material. The flow was described by a nonlinear Brinkman–Forchheimer-extended Darcy equation. Kuznetsov [24] conducted an analytical study of the effect of thermal dispersion on fully developed forced convection in a parallel-plate channel partly filled with a fluid saturated porous medium. Kuznetsov [25] discussed the effect of roughness on turbulent flow in a composite porous/fluid duct. It was shown that roughness of the porous/fluid interface impacts turbulent flow in the clear fluid region as well as overall heat transfer in the duct.

In all of the above mentioned studies, the authors have focused on steady state flow and heat transfer phenomenons. However, in actual situations most of the flow phenomenons are unsteady in nature. Very little attention has been given to the unsteady problem for the composite channel flow problems. In this regard, Umavathi and Palaniappan [26] investigated the unsteady flow of a viscous fluid in a stratum. Umavathi et al. [27] considered the unsteady flow and heat transfer of a viscous fluid in a horizontal composite channel with oscillatory injection velocity and presented an analytic solution.

The purpose of the present study is to investigate the effect of oscillatory injection velocity on the unsteady flow and heat transfer in a composite porous annulus. The inner half region that is attached to the inner cylinder is porous while the outer half region is filled with a clear fluid. Both the cylinders inject an oscillatory velocity to the fluid. Many notations used in this paper are taken from [27]. An analytical solution is presented based on two terms, i.e. harmonic and non-harmonic terms. The analysis made in this problem can be used to study phenomenons like filtration of water, petroleum engineering, and fault zone in geothermal systems.

2. Mathematical Formulation

Consider the unsteady, fully developed, laminar flow of an incompressible viscous fluid in an infinitely-long composite channel consisting of two concentric cylinders (see Fig.1).

The region $R_1 < r < (R_1 + R_2)/2$ is attached to the inner cylinder and is filled with a porous medium while the region $(R_1 + R_2)/2 < r < R_2$ is occupied by a clear viscous fluid. Both the cylinders are assumed to be infinite and placed horizontally; therefore all of the physical dependent variables except pressure are functions of r and t. Furthermore, the inner cylinder is held at constant temperature T_{w1}, while the outer cylinder is fixed at the temperature T_{w2} with $T_{w2} > T_{w1}$. Both the fluid and the porous region are in local thermal equilibrium. Moreover, the fluid flows in the channel due to a constant pressure gradient, and the heat transfer is due to the presence of a constant temperature difference $\Delta T = T_{w2} - T_{w1}$. Under the assumption mentioned above, the governing equations of motion and

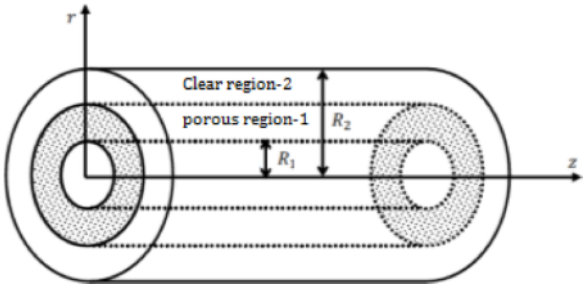

Fig. 1. Schematic flow configuration.

heat transfer are

$$\frac{u_i}{r}+\frac{\partial u_i}{\partial r}=0\,, \tag{1}$$

$$\rho\left(\frac{\partial w_i}{\partial t}+u_i\frac{\partial w_i}{\partial r}\right)=-\frac{\partial p}{\partial z}+\frac{\chi_\mu}{r}\frac{\partial}{\partial r}\left(r\frac{\partial w_i}{\partial r}\right)-\chi\frac{\mu}{s}w_i\,, \tag{2}$$

$$\rho C_p\left(\frac{\partial T_i}{\partial t}+u_i\frac{\partial T_i}{\partial r}\right)=\chi_k\frac{\partial^2 T_i}{\partial r^2}+\frac{\chi_k}{r}\frac{\partial T_i}{\partial r}+2\chi_\mu\left(\frac{\partial u_i}{\partial r}\right)^2+\chi_\mu\left(\frac{\partial w_i}{\partial r}\right)^2+2\chi_\mu\left(\frac{u_i}{r}\right)^2+\chi\frac{\mu}{s}w_i^2\,, \tag{3}$$

where $i=1,2$ gives equations for Regions 1 (porous region) and 2 (clear region), respectively; w_i is the axial and u_i the radial component of the fluid velocity and T_i is the temperature of the fluid, ρ, μ, and C_p are the fluid density, dynamic viscosity, and specific heat at constant pressure, respectively, while s is the permeability of porous medium. The other coefficients appearing in (1)–(3) are defined as

$$\chi=\begin{cases}1 \text{ for porous matrix region},\\ 0 \text{ for clear fluid region},\end{cases}$$

$$\chi_\mu=\begin{cases}\mu_{\text{eff}} \text{ for porous matrix region},\\ \mu \text{ for clear fluid region},\end{cases}$$

$$\chi_k=\begin{cases}k_{\text{eff}} \text{ for porous matrix region},\\ k \text{ for clear fluid region}.\end{cases}$$

We assume isothermal and no slip boundary conditions at surfaces and continuous velocity, shear stress, temperature, and heat flux at the interface.

It is assumed that the velocity and shear stress are continuous at the interface, unlike [15], where the jump condition was taken on the shear stress. It is

$$w_1(R_1)=0\,,\ \ w_2(R_2)=0\,, \tag{4}$$

$$w_1(R_m)=w_2(R_m),\ \text{where } R_m=\frac{R_1+R_2}{2}\,,\qquad \mu_{\text{eff}}\frac{\partial w_1}{\partial r}=\mu\frac{\partial w_2}{\partial r}\ \text{ at } r=R_m\,. \tag{5}$$

The thermal boundary and interface conditions for both fluids are given by

$$T_1(R_1)=T_{w1}\,,\ \ T_2(R_2)=T_{w2}\,,\ \ T_1(R_1)=T_2(R_2)\,, \tag{6}$$

$$K_{\text{eff}}\frac{\partial T_1}{\partial r}=K\frac{\partial T_2}{\partial r}\ \text{ at } r=R_m\,. \tag{7}$$

The mass conservation law (1) gives that u_1 and u_2 are depending on r and t. Therefore we take

$$u_i=\frac{f(t)}{r},\ \ u_i=\frac{u_0R_1(1+\varepsilon A\,\mathrm{e}^{\mathrm{i}\omega t})}{r}\,, \tag{8}$$

where ω is the frequency parameter, A a real positive constant, and ε the amplitude such that $\varepsilon A\le 1$.

Introducing non-dimensional variables

$$r^*=\frac{ru_0}{\upsilon}\,,\ \ w_i^*=\frac{w_i}{u_0}\,,\ \ t^*=\frac{tu_0^2}{\upsilon}\,,\ \ \theta=\frac{T-T_{w_2}}{T_{w_1}-T_{w_2}}\,, \tag{9}$$

where u_0 is the reference velocity. Using (9) and dropping asterisks, (2) and (3) in dimensionless form become

$$\frac{\partial w_i}{\partial t}+\frac{\mathrm{Re}(1+\varepsilon A\,\mathrm{e}^{\mathrm{i}\omega t})}{r}\frac{\partial w_i}{\partial r}=-P+C_i\frac{\partial^2 w_i}{\partial r^2}+\frac{C_i}{r}\frac{\partial w_i}{\partial r}-\chi\sigma^2 w_i\,, \tag{10}$$

$$\frac{\partial \theta_i}{\partial t}+\frac{\mathrm{Re}(1+\varepsilon A\,\mathrm{e}^{\mathrm{i}\omega t})}{r}\frac{\partial \theta_i}{\partial r}=B_i\frac{\partial^2\theta_i}{\partial r^2}+\frac{B_i}{r}\frac{\partial\theta_i}{\partial r}+4\frac{C_i\mathrm{Re}^2\mathrm{Ec}(1+\varepsilon A\,\mathrm{e}^{\mathrm{i}\omega t})^2}{r^4}+\mathrm{Ec}C_i\left(\frac{\partial w_i}{\partial r}\right)^2+\chi\mathrm{Ec}\sigma^2 w_i^2\,, \tag{11}$$

where $i=1,2$ gives equations for porous and non-porous space, respectively, and $C_1=m$, $C_2=1$, $B_1=k/\mathrm{Pr}$, $B_2=1/\mathrm{Pr}$, $P=\mu/(\rho^2u_0^3)\partial p/\partial z$, $\sigma^2=\nu^2/(su_0^2)$. $\mathrm{Pr}=(\rho\upsilon C_p)/k$ is the Prandtl number, $m=\mu_{\text{eff}}/\mu$ the ratio of viscosities, and $k=K_{\text{eff}}/K$ the ratio of thermal conductivities; $\mathrm{Ec}=u_0^2/C_p\Delta T$ is the Eckert number and $\mathrm{Re}=R_1u_0/\upsilon$ the Reynold number.

The non-dimensional form for the boundary and interface conditions reduce to

$$w_1(R_1)=0\,,\ \ w_2(R_2)=0\,,\qquad \theta_1(R_1)=1\,,\ \ \theta_2(R_2)=0\,, \tag{12}$$

$$w_1(R_m)=w_2(R_m)\,,\ \ \theta_1(R_m)=\theta_2(R_m)\,, \tag{13}$$

$$m\frac{\partial w_1}{\partial r}|r=R_m=\frac{\partial w_2}{\partial r}|r=R_m\,,\qquad k\frac{\partial\theta_1}{\partial r}|r=R_m=\frac{\partial\theta_2}{\partial r}|r=R_m\,. \tag{14}$$

3. Solution of the Problem

The momentum and energy equations (10) and (11) are coupled partial differential equations that cannot be solved in closed form. However, they can be reduced

to a set of ordinary differential equations that can be solved analytically by expanding the series for velocity and temperature fields as

$$w_i(r,t) = w_{i0}(r) + \varepsilon\, e^{i\omega t} w_{i1}(r) + O(\varepsilon^2) + \ldots, \quad i = 1,2 \tag{15}$$

$$\theta_i(r,t) = \theta_{i0}(r) + \varepsilon\, e^{i\omega t} \theta_{i1}(r) + O(\varepsilon^2) + \ldots, \quad i = 1,2\,. \tag{16}$$

This is a valid assumption because of the choice of u_i as defined in (8) and that the amplitude $\varepsilon A \leq 1$. By substituting (15) and (16) into (10) to (11), equating the harmonic and non-harmonic terms, and neglecting the higher-order terms of $O(\varepsilon^2)$, one can obtain the following pairs of equations for (u_{i0}, θ_{i0}) and (u_{i1}, θ_{i1}):

Non-Periodic Coefficients $O(\varepsilon^0)$

$$C_i \frac{\partial^2 w_{i0}}{\partial r^2} + \frac{(C_i - \mathrm{Re})}{r} \frac{\partial w_{i0}}{\partial r} - \chi \sigma^2 w_{i0} = P, \tag{17}$$

$$B_i \frac{\partial^2 \theta_{i0}}{\partial r^2} + \frac{(B_i - \mathrm{Re})}{r} \frac{\partial \theta_{i0}}{\partial r} + \frac{4 C_i \mathrm{Re}^2 \mathrm{Ec}}{r^4} + \mathrm{Ec} C_i \left(\frac{\partial w_{i0}}{\partial r} \right)^2 + \chi \mathrm{Ec} \sigma^2 w_{i0}^2 = 0\,. \tag{18}$$

Periodic Coefficients $O(\varepsilon^1)$

$$C_i \frac{\partial^2 w_{i1}}{\partial r^2} + \frac{(C_i - \mathrm{Re})}{r} \frac{\partial w_{i1}}{\partial r} - \chi \sigma^2 w_{i1} - i\omega w_{i1} - \frac{A\mathrm{Re}}{r} \frac{\partial w_{i0}}{\partial r} = 0\,, \tag{19}$$

$$B_i \frac{\partial^2 \theta_{i1}}{\partial r^2} + \frac{(B_i - \mathrm{Re})}{r} \frac{\partial \theta_{i1}}{\partial r} - i\omega \theta_{i1} - \frac{A\mathrm{Re}}{r} \frac{\partial \theta_{i0}}{\partial r} + \frac{8 C_i \mathrm{Ec} \mathrm{Re}^2 A}{r^4} + 2\mathrm{Ec} C_i \cdot \left(\frac{\partial w_{i0}}{\partial r} \right) \left(\frac{\partial w_{i1}}{\partial r} \right) + 2\chi \mathrm{Ec} \sigma^2 w_{i0} w_{i1} = 0\,. \tag{20}$$

Using (15) and (16), the boundary and interface conditions can be written as

$$w_{1i}(R_1) = 0\,, \quad w_{2i}(R_2) = 0\,, \quad w_{1i}(R_m) = w_{2i}(R_m)\,, \tag{21}$$

$$m \frac{\partial w_{1i}}{\partial r} = \frac{\partial w_{2i}}{\partial r} \quad \text{at } r = R_m\,, \tag{22}$$

$$\theta_{1i}(R_1) = 1 - \delta_{1i}\,, \quad \theta_{2i}(R_2) = 0\,, \tag{23}$$

$$\theta_{1i}(R_m) = \theta_{2i}(R_m)\,, \quad k \frac{\partial \theta_{1i}}{\partial r} = \frac{\partial \theta_{2i}}{\partial r} \quad \text{at } r = R_m\,, \tag{24}$$

where $i = 0,1$ gives the boundary and interface conditions for non-periodic $O(\varepsilon^0)$ and periodic $O(\varepsilon^1)$ coefficients, respectively; δ_{1i} is the Kronecker delta.

4. Results and Discussion

The nonlinear differential equations (17) – (20) with boundary conditions (21) – (24) are solved analytically. As the solutions of these equations are quite lengthy and complicated, therefore we are giving tabulated values for velocity, temperature, and their derivatives. These values are given in Table 1.

Table 1. Values of velocity w, temperature θ, and their derivatives by taking the values of r between 1 and 2, while $\sigma = 1/2$, $m = 1/4$, $P = -2$, $\omega = 5$, $\omega t = \pi/3$, $k = 0.25$, $\mathrm{Ec} = 1$, $\mathrm{Pr} = 1$, $\varepsilon A = 0.2$, $\mathrm{Re} = 1$ are kept fixed.

r	w	w'	θ	θ'
1	$5.0610 \cdot 10^{-21}$	1.74912	1.0	0.509117
1.1	0.163302	1.50011	1.02005	−0.107671
1.2	0.296212	1.13674	0.978537	−0.721948
1.3	0.385923	0.631519	0.875794	−1.33288
1.4	0.416864	−0.04322	0.711444	−1.96136
1.5	0.370724	−0.91452	0.480286	−0.67267
1.6	0.337674	−0.43261	0.407571	−0.780192
1.7	0.28416	−0.63783	0.324296	−0.886192
1.8	0.210079	−0.84391	0.229949	−1.00366
1.9	0.115365	−1.05041	0.122795	−1.14417
2.0	$-1.443 \cdot 10^{-10}$	−1.25683	$2.458 \cdot 10^{-9}$	−1.31811

The effects of various physical parameters are analyzed by plotting graphs.

Figures 2 and 3 display the effect of the porous medium parameter σ on the velocity and temperature profiles, respectively. It is noticed from the figures that as σ increases the velocity and temperature profiles decrease. This is because of the shrinking of the pores area due to which momentum transport reduces and as a result, velocity as well as temperature profile decreases. It is also observed from here that σ has significant effects in both porous and non-porous regions and the velocity profile reduces in both regions; however, this reduction is more significant in the porous region.

The effects of the viscosity ratio parameter m on the velocity and temperature profiles are shown in Figures 4 and 5, respectively. As m increases, the velocity profile decreases and the temperature profile increases. This conduct of the flow is due to the increasing field

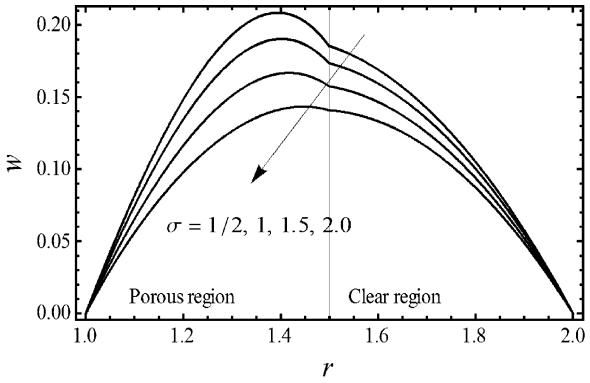

Fig. 2. Velocity profiles for different values of the porous medium parameter σ, when $m = 1/4$, $P = -1$, $\omega = 5$, $\omega t = \pi/3$, $\mathrm{Re} = 1$ are kept fixed.

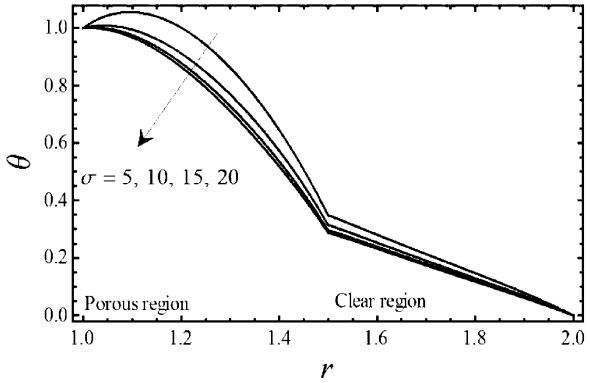

Fig. 3. Temperature profiles for different values of the porous medium parameter σ, when $m = 1/4$, $P = -1$, $\omega = 5$, $\omega t = \pi/3$, $\mathrm{Re} = 1$ are kept fixed.

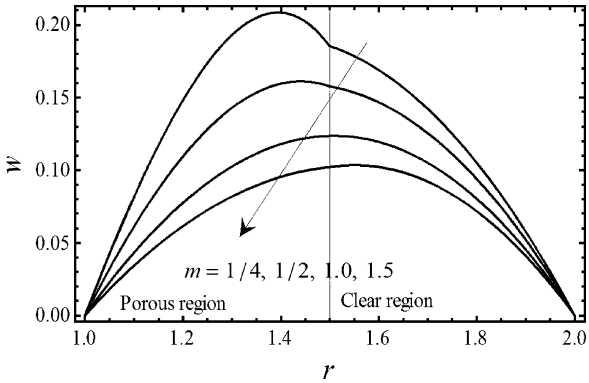

Fig. 4. Velocity profiles for different values of the ratio of the viscosities m, when $\sigma = 1/2$, $P = -1$, $\omega = 5$, $\omega t = \pi/3$, $\mathrm{Re} = 1$ are kept fixed.

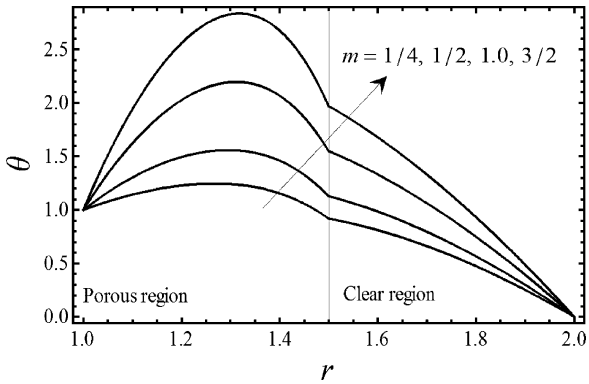

Fig. 5. Temperature profiles for different values of the ratio of the viscosities m, when $m = 1/4$, $P = -1$, $\omega = 5$, $\omega t = \pi/3$, $\mathrm{Re} = 2$, $k = 0.25$, $\mathrm{Ec} = 1.0$, $\mathrm{Pr} = 1$, $\sigma = 1$ are kept fixed.

viscosity by which the process of internal heat generation enhances, and due to thickening fluid the velocity profile decreases. It is worth mentioning here that the decrease in velocity profile in the porous region is more prominent as compared to the clear region. Similarly, the increase in temperature profile by increasing m is more significant in the porous region. This is due to the presence of a resistive force which amplifies the temperature and reduces the velocity more significantly as compared to the clear region.

Figure 6 depicts the effect of the Prandtl number Pr on the temperature profile. From the figure it is observed that the temperature profile increases as Pr increases. This conduct of the temperature profile is due to increasing viscous diffusion in the presence of viscous dissipation which enhances internal heat generation in the annulus.

Figure 7 shows the graph of the temperature profile for different values of thermal conductivity k. The temperature profile also decreases for the porous region for the increase of k and remains constant for the clear region in the fluid.

Figure 8 shows the effect of the Eckert number Ec on the temperature profile. As Ec increases the temperature profile also increases which is due to the increase of fluid frictional effects.

Figures 9 and 10 give the effect of the amplitude of oscillation εA on the velocity and temperature fields, respectively. We take the oscillation amplitude to be small for analytical solutions, i.e. $\varepsilon A \leq 1$, and $\varepsilon A = 0$ corresponds to the steady state solution. It is clear from Figure 9 that as we increase the amplitude, the velocity decreases for the porous region but remains constant for the clear region. On the other hand, an increase

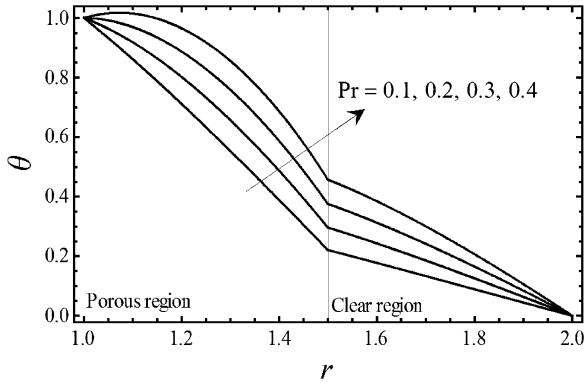

Fig. 6. Temperature profiles for different values of the Prandtl number Pr, when $m = 1/4$, $P = -1$, $\omega = 5$, $\omega t = \pi/3$, Re $= 2$, $k = 0.25$, Ec $= 1.0$, Pr $= 1$, $\sigma = 1$ are kept fixed.

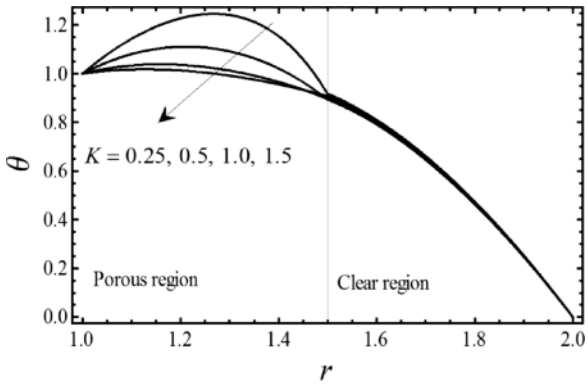

Fig. 7. Temperature profiles for different values of the conductivities k, when $m = 1/4$, $P = -1$, $\omega = 5$, $\omega t = \pi/3$, Re $= 2$, $k = 0.25$, Ec $= 1.0$, Pr $= 1$, $\sigma = 1$ are kept fixed.

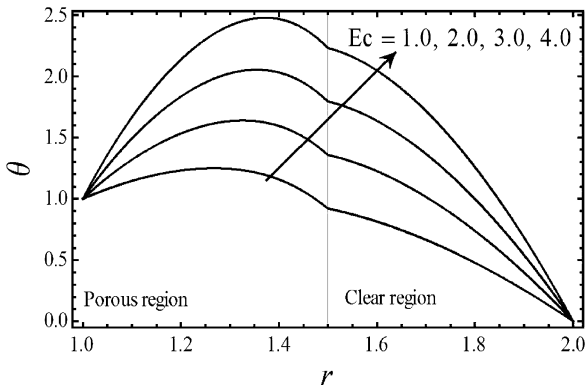

Fig. 8. Temperature profiles for different values of the Eckert number Ec, when $m = 1/4$, $P = -1$, $\omega = 5$, $\omega t = \pi/3$, Re $= 2$, $k = 0.25$, Ec $= 1.0$, Pr $= 1$, $\sigma = 1$ are kept fixed.

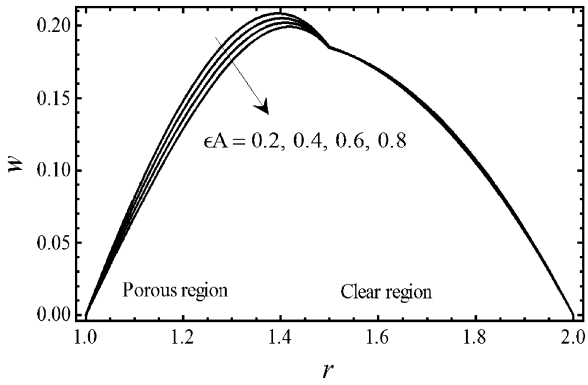

Fig. 9. Velocity profiles for different values of the oscillation amplitude εA, when $\sigma = 1/2$, $m = 1/4$, $P = -1$, $\omega = 5$, $\omega t = \pi/3$, Re $= 1$ are kept fixed.

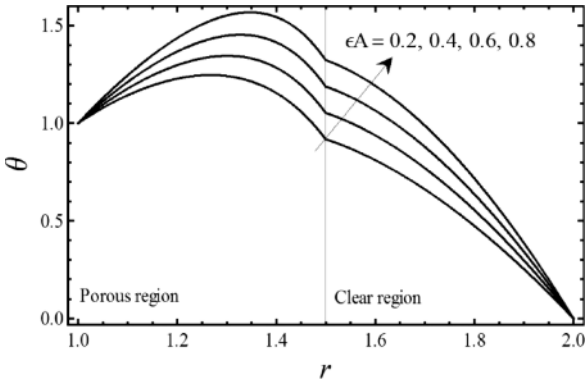

Fig. 10. Temperature profiles for different values of the oscillation amplitude εA, when $m = 1/4$, $P = -1$, $\omega = 5$, $\omega t = \pi/3$, Re $= 2$, $k = 0.25$, Ec $= 1.0$, Pr $= 1$, $\sigma = 1$ are kept fixed.

in amplitude has an increasing effect on the temperature profile for both the region of the channel, which is a quite expected behaviour of the profile.

Figures 11 and 12 show the effects of pressure on the velocity and temperature profile. Both the velocity and the temperature increase as the pressure decreases, which is expected because of favourable pressure.

Figures 13 and 14 show the effects of angular frequency ω on both the velocity and the temperature. When we increase ω, velocity increases while temperature decreases.

Figures 15 and 16 show the effect of the Reynolds number Re on velocity and temperature profiles. The velocity decreases by increasing Re due to the decreasing inertial forces, while temperature increases by an increase of Re.

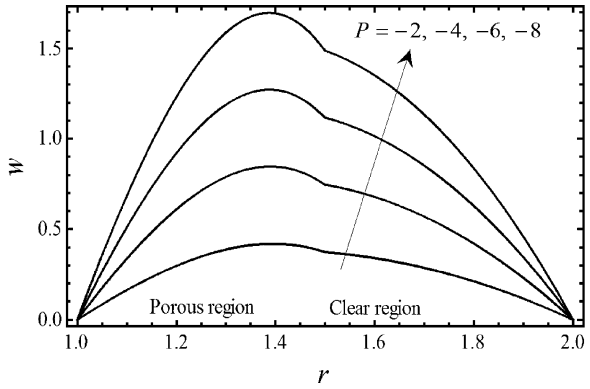

Fig. 11. Velocity profiles for different values of the pressure P, when $\sigma = 1/2$, $m = 1/4$, $\omega = 5$, $\omega t = \pi/3$, Re $= 1$ are kept fixed.

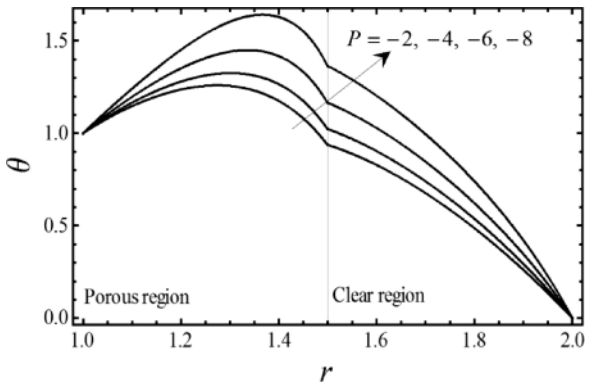

Fig. 12. Temperature profiles for different values of the pressure P, when $m = 1/4$, $P = -1$, $\omega = 5$, $\omega t = \pi/3$, Re $= 2$, $k = 0.25$, Ec $= 1.0$, Pr $= 1$, $\sigma = 1$ are kept fixed.

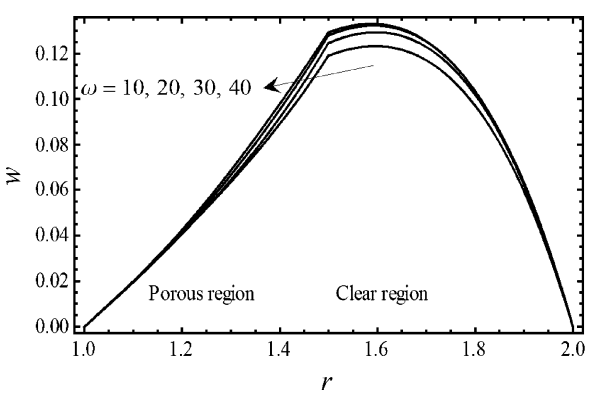

Fig. 13. Velocity profiles for different values of the frequency ω, when $\sigma = 1/2$, $m = 1/4$, $\omega t = \pi/3$, $P = -1$, Re $= 5$ are kept fixed.

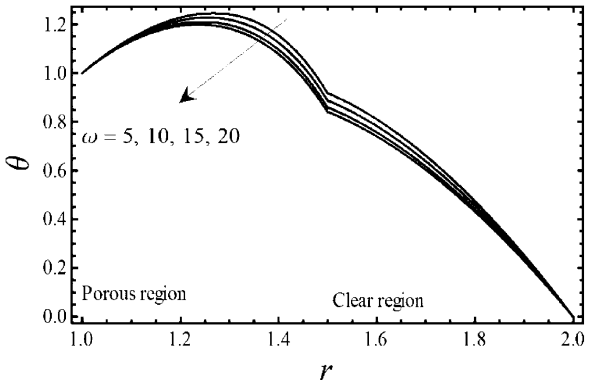

Fig. 14. Temperature profiles for different values of the frequency ω, when $m = 1/4$, $P = -1$, $\omega = 5$, $\omega t = \pi/3$, Re $= 2$, $k = 0.25$, Ec $= 1.0$, Pr $= 1$, $\sigma = 1$ are kept fixed.

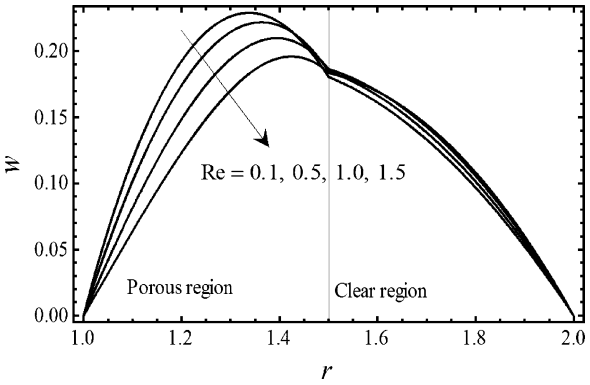

Fig. 15. Velocity profiles for different values of the Reynolds number Re, when $\sigma = 1/2$, $m = 1/4$, $\omega = 5$, $\omega t = \pi/3$, $P = -1$ are kept fixed.

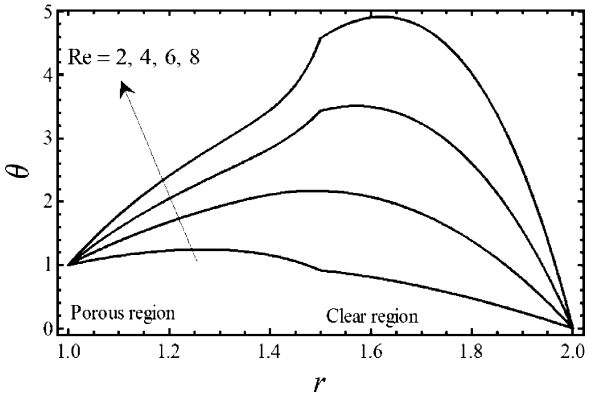

Fig. 16. Temperature profiles for different values of the Reynolds number Re, when $m = 1/4$, $P = -1$, $\omega = 5$, $\omega t = \pi/3$, $k = 0.25$, Ec $= 1.0$, Pr $= 1$, $\sigma = 1$ are kept fixed.

5. Conclusion

An unsteady flow of a viscous fluid between two concentric cylinders whose half space is filled with a porous medium is analyzed analytically. Taking viscous dissipation into account, the heat transfer analysis is also made for both regions of the permeable channel. The computed solutions are plotted graphically for different values of parameters and the following concluding observations are noticed from the above analysis:

- It is concluded that by increasing the permeability of pores the velocity as well as temperature profile decrease in both regions of the channel. However, this decrease is more significant in the porous region.
- The velocity profile decreases as the viscosity ratio parameter increases, although this decrease is prominent in the lower region. On the other hand, the temperature profile exhibits an inverse behaviour of the said parameter.
- The temperature profile is an increasing function of Prandtl number and Eckert number while for the thermal conductivity the temperature profile decreases.
- It is noted that the amplitude in the velocity decreases for the porous region and remains constant for the clear region while the temperature profile is an increasing function for amplitude.
- Both the velocity and the temperature are increasing functions of pressure.
- It is observed that the velocity increases by an increase of angular frequency while the temperature decreases.
- By increase of Reynolds number the velocity decreases while the temperature increases.

[1] A. S. Berman, J. Appl. Phys. **24**, 1232 (1953).
[2] R. M. Terrill, Aeronaut. Quart. **15**, 299 (1964).
[3] F. M. Skalak and C. Y. Wang, Siam J. Appl. Math. **34**, 535 (1978).
[4] R. M. Terrill and P. W. Thomas, Appl. Sci. Res. **21**, 37 (1969).
[5] R. M. Terrill and P. W. Thomas, Phys. Fluids. **16**, 356 (1973).
[6] F. Marques, J. Sanchez, and P. D. Weidman, J. Fluid. Mech. **374**, 221 (1998).
[7] C. L. Taylor, W. H. H. Banks, M. B. Zaturska, and P. G. Drazin, Quart. J. Mech. Appl. Math. **44**, 105 (1991).
[8] G. Neale and W. Nader, Cand. J. Chem. Eng. **52**, 475 (1974).
[9] D. A. Nield, S. L. M. Junqueira, and J. L. Lage, J. Fluid. Mech. **322**, 201 (1996).
[10] A. K. Al-Hadhrami, L. Elliott, and D. B. Ingham, Trans. Porous. Media **49**, 265 (2002).
[11] S. Kim and W. B. Russell, J. Fluid Mech. **154**, 269 (1985).
[12] D. A. Nield, A. V. Kuznetsov, and M. Xiong, Trans. Porous. Media **56**, 351 (2004).
[13] K. Hooman, H. Gurgenci, and A. A. Merrikh, Int. J. Heat Mass Transfer **50**, 2051 (2007) .
[14] A. V. Kuznetsov, Appl. Sci. Res. **56**, 53 (1996).
[15] A. V. Kuznetsov, Int. Commun. Heat Mass Transfer **24**, 401 (1997).
[16] A. V. Kuznetsov, Int. J. Heat Mass Tranfer **41**, 2556 (1998).
[17] A. V. Kuznetsov, Acta Mech. **140**, 163 (2000).
[18] M. A. Al-Nimr and A. F. Khadrawi, Porous Media **51**, 157 (2003).
[19] D. S. Chauhan and V. Kumar, Turkish J. Eng. Env. Sci. **33**, 91 (2009).
[20] D. S. Chauhan and R. Agrawal, Chem. Eng. Commun. **197**, 848 (2010).
[21] D. S. Chauhan and P. Rastogi, App. Math. Sci. **4**, 643 (2010).
[22] D. S. Chauhan and V. Kumar, Appl. Math. Sci. **4**, 2683 (2010).
[23] A. V. Kuznetsov, Z. Angew. Math. Phys. **52**, 135 (2001).
[24] A. V. Kuznetsov, Int. J. Thermal Sci. **43**, 1047 (2004).
[25] A. V. Kuznetsov, Flow Turbul. Combust. **60**, 173 (1998).
[26] J. C. Umavathi and D. Palniappan, J. Appl. Mech. **69**, 35 (2000).
[27] J. C. Umavathi, A. J. Chamkha, A. Mateen, and A. Al-Mudhaf, Nonlinear Anal. Mod. Cont. **14**, 397 (2009).